Articles

Coupling Octupoles in Crystals: The Case of the 1,3,5-Trinitrobenzene−Triphenylene 1:1 Molecular Co-Crystal

Joseph Zyss,*,† Isabelle Ledoux-Rak,† Hans-Christoph Weiss,‡ Dieter Bläser,‡ Roland Boese,‡ Praveen K. Thallapally,§ Venkat R. Thalladi,§ and Gautam. R. Desiraju§

Laboratoire de Photonique Quantique et Moléculaire (UMR 8537), Institut d'Alembert (IFR 121), Ecole Normale Supérieure de Cachan, 61 Avenue du Président Wilson 94235 Cachan Cedex France, Institut für Anorganische Chemie, Universität-GH Essen, Universitätstrasse 5-7, D-45177, Essen, Germany, and School of Chemistry, University of Hyderabad, Hyderabad 500 046, India

Received January 15, 2003. Revised Manuscript Received March 10, 2003

A new supramolecular crystal engineering approach toward quadratic nonlinear optics is inferred from an acentric cocrystalline template made of two different bi-dimensional octupolar molecules: trinitrobenzene (TNB) and triphenylene (TP). The resulting 2-D octupolar cocrystalline lattice is proposed as a generic template toward multipolar crystalline engineering studies. X-ray diffraction data evidence parallel stacks with alternating vertically overlapping TNB and TP units, leading to a significant $\pi-\pi$ intermolecular charge transfer which cannot be accounted for by an oriented gas model.

Introduction

Classically, engineering of molecular materials toward quadratic nonlinear optical applications rests mainly on two strongly interconnected principal steps. These steps are, respectively, molecular and supramolecular in concept.[1] The first one consists of identification and synthesis of optimal molecular building blocks that can sustain an enhanced (hyper)polarizability response, measured at this molecular level in solution by well-tried experimental tools such as electric field second-harmonic generation (EFISH[2]) or harmonic light scattering (HLS)[3] techniques.

In this context, donor−acceptor π electron systems, sometimes referred to under the generic name of molecular diodes, and derived from the basic *p*-nitroaniline (pNA) blueprint, have emerged as a first generation paradigm. A simple two-level quantum model extrapolating to higher-order Mulliken's linear approach to charge transfer satisfactorily accounts for the order of magnitude and frequency dispersion of the quadratic nonlinear properties of such quasi 1-D systems, providing the optical properties of this family with robust and predictive conceptual foundations.[1−2]

The second step toward quadratic nonlinear optical applications is based on crystal engineering and consists of the subsequent macroscopic organization of microscopic molecular building blocks into a noncentrosymmetric crystal packing.[4] To achieve macroscopic departure from centrosymmetry, two major avenues have been followed so far in the realm of dipolar chromophore units of the pNA type, namely single crystals on one hand and thermally assisted electric field poling on the other. In the former case, the chromophore can be designed to bear a chiral substituent [e.g., derivative of proline in the case of *N*-4-nitrophenyl-(L)-prolinol (NPP)[5] or of alanine for methyl(2,4-dinitrophenyl) aminopropanoate (MAP)[6]] which is bound to enforce formation of a noncentrosymmetric lattice. Other strategies have called upon the minimization of the dipole moment as in the case of 3-methyl-4-nitropyridine-1-oxide (POM),[7]

* To whom correspondence should be addressed via e-mail: Zyss@lpqm.ens-cachan.fr.
† Ecole Normale Supérieure de Cachan.
‡ Universität-GH Essen.
§ University of Hyderabad.

(1) Zyss, J., Ed. *Molecular Nonlinear Optics: Materials, Physics and Devices*; Academic Press: New York, 1994. Nalwa, H., Miyata, S., Eds. *Nonlinear Optics of Organic Molecules and Polymers*; CRC Press: New York, 1996. Desiraju, G. R., Ed. *Crystal Engineering*; Elsevier Science: New York, 1989; Chapter 8 and references therein. Günter, P., Ed. *Nonlinear Optical Effects and Materials*; Springer Series in Optical Sciences; Springer: New York, 2000. Zyss, J. Ed. *Molecular Photonics: Materials, Physics and Devices*; C. R. Physique, Elsevier and Académie des Sciences: Paris, 2002; vol. 3 (4).

(2) Oudar, J.-L. *J. Chem. Phys.* **1977**, *67*, 446. Levine, B. F.; Bethea, C. G. *J. Chem. Phys.* **1975**, *63*, 2666. Ledoux, I.; Zyss, J. *Chem. Phys.* **1982**, *73*, 203.

(3) Terhune, R. W.; Maker, P. D.; Savage, C. M. *Phys. Rev. Lett.* **1965**, *14*, 681. Clays, K.; Persoons, A. *Phys. Rev. Lett.* **1991**, *66*, 2980. Zyss, J.; ChauVan, T.; Dhenaut, C.; Ledoux, I. *Chem. Phys.* **1993**, *177*, 281. Ray, P. C.; Das, P. K. *J. Chem. Phys.* **1995**, *9*, 9, 17891.

(4) Oudar, J. L.; Zyss, J. *Phys. Rev. A* **1982**, *26*, 2016. Zyss, J.; Oudar, J. L. *Phys. Rev. A* **1982**, *26*, 2028.

(5) Zyss, J.; Nicoud, J. F.; Coquillay, M. *J. Chem. Phys.* **1984**, *81*, 4160.

(6) Oudar, J−L.; Hierle, R. *J. Appl. Phys.* **1977**, *48*, 2699.

10.1021/cm031018m CCC: $25.00
Published on Web 07/19/2003

entailing the benefit of weakening the disruptive influence of dipole−dipole interactions that would otherwise favor antiparallel stacking of dipolar units. Finally, organo-mineral ionic crystals such as those built-up from the cocrystallization in an acid environment of cationic NLO chromophores anchored to a poly-anionic scaffold (such as 2-amino-5-nitropyridine dihydrogenphosphate or chlorate (2A5NPDP or 2A5NPCl))[8] have been proposed and elaborated. In this avenue, the ease of counterion exchange techniques has added a fruitful dose of versatility as had been initially proposed by Meredith.[8] Such an approach can be also applied to purely organic ionic crystal arrangements (2A5NP tartrate).[9] Indeed, record-high nonlinear coefficients up to a few hundreds of pm/V have been achieved throughthis strategy in crystals such as SPCD[10] or 4-*N*,*N*-dimethylamino-4′-*N*′-methyl-stilbazolium tosylate (DAST)[11] as a result of the elongated and highly polarizable nature, as well as quasi perfect alignment, in the crystal lattice of cationic stilbene-like chromophores.

Another avenue which is complementary to that followed in this work is based on guest−host incorporation or tethering of chromophores to polymer matrixes with the possibility of subsequently imparting a statistical polar order by external electric field poling. The processibility of polymers in multilayer thin films over large areas by soft lithography techniques[12] promises cost reduction and high-volume production, which makes this approach appealing for industrial developments.[13] Some current efforts to combine the benefits of polymer thin-film technology and ordering of crystals seem to designate nanocrystalline structures nested in a polymer host as an interesting compromise and a possible target for future applications.[13,14]

As opposed to this single bipolar blueprint, multipolar design rules target the more complex 2- and 3-D substitution patterns made-up of donor and acceptor groups attached to a variety of conjugated or semiconjugated spatially extended networks (such as paracyclophanes where a through-space charge transfer between the two phenyl moieties has been recently evidenced[15]). Such higher-dimensional templates with the alternated donor−acceptor cube and its projection along the main diagonals have been proposed and implemented since the early 1990s with the possibility of both central and lateral connectivity between active groups.[16] This approach has been seeded by the recognition of TATB as the simplest nonpolar noncentrosymmetric generalization of the earlier pNA template.[17] This rather serendipitous finding was subsequently developed and rationalized in a systematic way on the basis of combined tensorial symmetry and quantum mechanical considerations, wherefrom the concepts of multipolar nonlinearities emerged.[16,18] A still largely untapped reservoir of new molecular structures, whereby full use of stereochemical considerations can be exploited, is thus available. Such chromophores, referred to as octupoles, have led to the recognition of multipolar structures comprising both dipolar and octupolar components as the most general template. The balance between these two contributions can be quantitatively expressed as the nonlinear anisotropy ratio.[19]

The absence of a dipole moment in octupolar molecules precludes, in particular, electric field poling in host−guest polymer systems. Again, some similarities emerge with strategies employed for dipolar structures, namely "all-optical" poling in the context of statistically ordered polymer blends,[19,20] and single-crystal octupolar ordering toward perfectly ordered octupolar packing.[21,22]

The merits and demerits of both approaches appear to be very similar to those already outlined for dipolar systems: namely, potentially higher efficiency from optimized crystal lattices at the expense of ease of fabrication for crystals as opposed to better processibility for polymer films. However, with smaller figures of merit, optical poling entails the unique possibility to engineer any desired spatial distribution of optical properties by use of externally controllable encoding parameters such as the phase and polarization of the "write" beams.[19,23]

In this work, we concentrate on a new crystal engineering approach with 2-D trigonal octupoles as molecular building blocks. Our approach uses the complexation of trigonal donor−acceptor molecules to generate solids with NLO activity higher than that of the corresponding single component crystals. This new approach is exemplified by the noncentrosymmetric crystal structure of the 1:1 molecular complex 1,3,5-trinitrobenzene−triphenylene (see Scheme 1 for molecular structures),

(7) Zyss, J.; Chemla, D. S.; Nicoud, J−F. *J. Chem. Phys.* **1981**, *74*, 4800.

(8) Meredith, G. R. In *Nonlinear Optical Properties of Organic and Polymeric Materials*; Williams, D. J., Ed.; ACS Symposium Series 233, American Chemical Society: Washington, DC, 1983; Chapter 2, p 27. Masse, R.; Zyss, J. *Mol. Eng.* **1991**, *1*, 141; Khodja, S.; Josse, D.; Zyss, J. *J. Opt. Soc. Am. B.* **1998**, *15* (2), 751. Watanabe, O.; Noritake, T.; Okada, A.; Kurauchi, T. *J. Mater. Chem.* **1993**, *3*, 1053. Horiuchi, N.; Lefaucheux, F.; Ibanez, A.; Josse, D.; Zyss, J. *J. Opt. Soc. Am. B* **2002**, *19* (8), 1830.

(9) Zyss, J.; Masse, R.; Bagieu-Beucher, M.; Lévy, J. P. *Adv. Mater.* **1993**, 5, 120.

(10) Bhowmik, A.; Dharmadhikari, A.; Thakur, M. *Observation of Spectral Narrowing and Mirrorless Lasing in SPCD*. Paper presented at CLEO 99, Baltimore, MD; Paper CThQ5, 1999.

(11) Marder, S. R.; Perry, J. W.; Schäfer, W. P. *Science* **1989**, *245*, 626;. Knoepfle, R.; Schlesser, R.; Ducret, R.; Guenter, P. *Nonlinear Opt.* **1995**, *9*, 143. Thakur, M.; Xu, J.; Bhowmik, A.; Zhou, L. *Appl. Phys. Lett.* **1999**, *74*, 635−637. Kawase, K.; Mizuno, M.; Sohma, S.; Takahashi, H.; Taniuchi, T.; Urata, Y.; Wada, S.; Tashiro, H.; Ito, H. *Optics Lett.* **1999**, *24*, 1065−1067.

(12) Brittain, S.; Paul, K.; Zhao, X.-M.; Whitesides, G. *Physics World* **1998**, *11*, 31−36. Bao, Z.; Rogers, J. A.; Katz, H. E. *J. Mater. Chem.* **1999**, *9*, 1905.

(13) Miyata, S., Sasabe, H., Eds. *Poled Polymers and their Applications to SHG and EO Devices*. Gordon and Breach: Amsterdam, The Netherlands, 1997.

(14) Ibanez, A.; Maximov, S.; Guiu, A.; Chaillout, C.; Baldeck, P. L. *Adv. Mater.* **1998**, *10*, 1540−1543. Thalladi, V. R.; Whitesides, G. M. *J. Am. Chem. Soc.* **2002**, *124*, 3520−3521.

(15) Zyss, J.; Ledoux, I.; Volkov, S. N.; Chernyak, V.; Mukamel, S.; Bartholomew, G. P.; Bazan, G. C. *J. Am. Chem. Soc.* **2000**, *122*, 11956. Bartolomew, G. P.; Ledoux, I.; Mukamel, S.; Bazan, G. C.; Zyss, J. *J. Am. Chem. Soc.* **2002**, *124*, 13480.

(16) Zyss, J. *J. Chem. Phys.* **1993**, *98*, 6583−6599. Zyss, J. *Nonlinear Optics* **1991**, *1*, 3−18.

(17) Ledoux, I.; Zyss, J.; Siegel, J. S.; Brienne, J.; Lehn, J. M. *Chem. Phys. Lett.* **1990**, *172*, 440.

(18) Zyss, J.; Ledoux, I. *Chem. Rev.* **1994**, *94*, 77−105.

(19) Brasselet, S.; Zyss, J. *J. Opt. Soc. Am. B* **1998**, *15*, 1, 208−210.

(20) Fiorini, C.; Charra, F.; Nunzi, J−M.; Samuel, I. D. W.; Zyss, J. *Opt. Lett.* **1995**, *20*, 2469.

(21) Braga, D.; Grepioni, F.; Desiraju, G. R. *Chem. Rev.* **1998**, *98*, 1375.

(22) Cho, B. R.; Lee, S. J.; Lee, S. H.; Son, K. H.; Kim, Y. H.; Doo, J.-Y.; Lee, G. J.; Kang, T. I.; Lee, Y. K.; Cho, M.; Jeon, S.-J. *Chem. Mater.* **2001**, *13* (5), 1438−1440.

(23) Donval, A.; Toussaere, E.; Brasselet, S.; Zyss, J. *Opt. Mater.* **1999**, *12*, 215.

Scheme 1. Structures of Trinitrobenzene (TNB), Triphenylene (TP), and Trimethylisocyanurate (TMI)

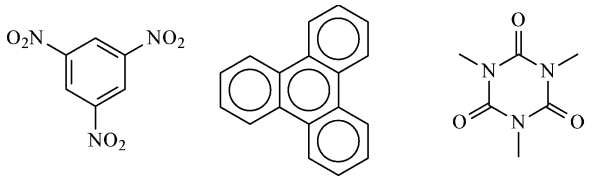

henceforth referred to as TNB−TP. In this structure, the two constituent units are strictly planar octupolar molecules with D_{3h} symmetry. An earlier attempt in this direction had been the 1:1 TNB−trimethyl isocyanurate (TMI) molecular complex. The major difference between TNB−TP and TNB−TMI is that the nonplanarity of the TMI octupole entails pronounced variations in the NLO properties. (TMI is considered nonplanar because of the out-of-plane arrangement of methyl H-atoms in the TMI−TNB complex. The nitro groups of TNB lie within the aromatic rings in the TNB−TP complex and hence TNB is considered planar in the present context.)

As is common in the crystal structures of $\pi-\pi$ donor acceptor complexes, TNB−TP consists of parallel stacks formed with alternating and well-overlapped TNB and TP molecules leading to significant intermolecular $\pi-\pi$ charge transfer. The TNB−TP structure thus embodies the following unique features to be developed in the following discussion: a noncentrosymmetric lattice made up of an alternating couple of octupolar subunits, and the possibility of intermolecular charge transfer which cannot be accounted for by a simple oriented gas tensorial model.

This crystal exemplifies a way toward the so-far largely elusive issue of intrastack plane-to-plane ordering in 2-D octupolar crystal engineering. We note here that there is a precedent for intralamellar plane-to-plane ordering. Complementary hydrogen bonds in the crystal structure of melamine−barbituric acid are of the intralamellar or lateral type and provide a solution for octupolar in-plane organization.[24] In contrast, earlier attempts to implement plane-to-plane interlocking has so far led only to limited SHG efficiencies.[25]

We begin in the following section with the description of the main structural features of TNB−TP as obtained from single-crystal X-ray diffraction data. The octupolar order is analyzed and dissected in terms of two basic H-bonded supramolecular synthons, which are identified as the up-scaling cornerstones responsible for the promotion of octupolar microscopic order into the crystalline supramolecular level. We discuss in detail the connection between structural data and the nonlinear optical properties of TNB−TP based on preliminary experimental data from NLO experiments in solution and powder. A tensorial model designed to account for intermolecular interactions along the stacking direction backs the discussion. A summary of the main results from this investigation, as well as perspectives for ongoing and future work, are outlined in the Conclusion.

Results and Discussion

Structure of the 1:1 Complex of 1,3,5-Trinitrobenzene and Triphenylene (TNB−TP). Tables 3 and 4 in Appendix A provide details of the crystallographic data which are discussed hereafter. The space group is $P2_1$ and the asymmetric unit contains a pair of TNB and TP units. As shown in Figure 1, these molecules are stacked nearly parallel to each other (0.59° dihedral angle between the molecular planes to form a diad). As is common in $\pi-\pi$ donor acceptor complexes, the diads are translated along the stack axis (in this case, the *a*-axis) leading to two distinct perpendicular distances (3.39 and 3.36 Å) between donor and acceptor moieties.[26] In the present case the centroïd-offset distances are 3.58, 1.16 (intradiad) and 3.62, 1.36 (interdiad) Å. This overall arrangement provides the major charge-transfer contribution in the system. The action of the 2_1-screw axis on this stacked column generates the entire crystal structure.

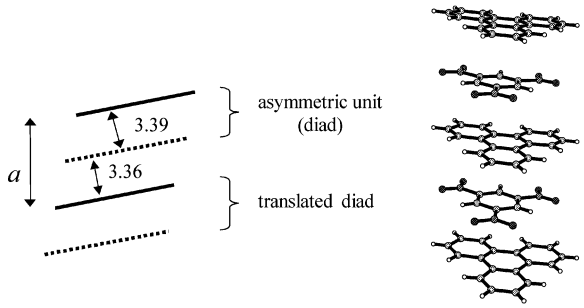

Figure 1. Two distinct donor-to-acceptor arrangements in the stack of alternating TNB and TP molecules in the title complex.

The adoption of a noncentrosymmetric space group by the title molecular complex is noteworthy in view of the more common centro symmetric packing in donor−acceptor complexes, and indeed in molecular complexes in general. A search of the Cambridge Structural Database (CSD, Version 5.21)[27] showed that of the 414 molecular complexes formed by seven common acceptors,[28] only 37 are noncentrosymmetric. In the present context, noncentrosymmetric packing is an attribute of not only the molecular complex TNB−TP, but also each of the constituents in their native structures[29,30] which is quite unusual. A possibly related point here is the C_3 molecular symmetry (in both TNB and TP) that is known to lead to a preference for noncentrosymmetric packing.[31]

There are several additional features of interest in terms of (a) weak hydrogen bonds and the supramolecular synthons formed thereby; (b) networks that are

(24) Choi, I. S.; Li, X.; Simanek, E. E.; Akaba, R.; Whitesides, G. M. *Chem. Mater.* **1999**, *11*, 684−690.
(25) Thalladi, V. R.; Brasselet, S.; Weiss, H−C.; Bläser, D.; Katz, A. K.; Carrell, H. L.; Boese, R.; Zyss, J.; Nangia, A.; Desiraju, G. R. *J. Am. Chem. Soc.* **1998**, *120*, 2563.
(26) Foster, R. *Organic Charge-Transfer Complexes.* Academic: New York, 1969.
(27) Allen, F. H.; Kennard, O. *Chem. Des. Autom. News* **1993**, *8*, 1.
(28) The seven acceptors are TNB, TCNQ, bis(ethylenedithio)-tetrathiafulvalene, 2,2′-bi-1,3-dithiole, pyromellitic dianhydride, mellitic trianhydride, and benzoquinone derivatives (mainly chloranil and DDQ).
(29) Ahmed, F. R.; Trotter, J. *Acta Crystallogr.* **1963**, *16*, 503.
(30) Choi, C. S.; Abel, J. E. *Acta Crystallogr.* **1972**, *B28*, 193. TNB has been reported to crystallize in the centrosymmetric space group *Pbca*, but recently we have identified a noncentrosymmetric polymorph in space group $Pca2_1$. Thallapally, P. K.; Katz, A. K.; Carrell, H. L.; Desiraju,G. R. manuscript in preparation.
(31) Desiraju, G. R.; Krishna, T. S. R. *Mol. Cryst. Liq. Cryst.* **1989**, *159*, 277.

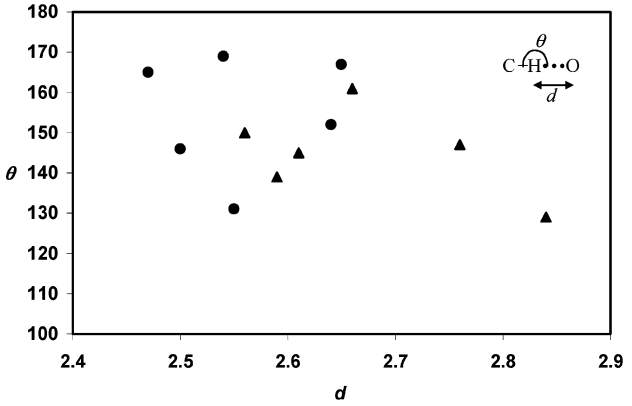

Figure 2. $d-\theta$ Plot (normalized) for the C−H···O hydrogen bonds in the title complex. Circles and triangles refer, respectively, to hydrogen bridges in synthon **I** and synthon **II**.

Scheme 2. Supramolecular Synthons Referred to in This Study

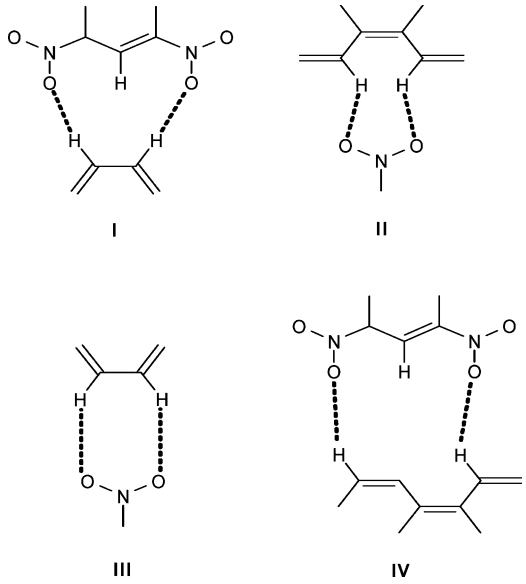

formed via the synthons and their interpenetration topology; and (c) comparison of the structure with that of the 1:1 complex formed by TNB and trimethyl isocyanurate, TMI.

Let us first consider the intermolecular C−H···O interactions. In light of earlier work on TNB−TMI[32] and other molecular complexes of TNB[33] it was expected that the structure of TNB−TP would also contain C−H···O hydrogen bonds. A distance−angle scatter plot of these interactions is given in Figure 2 from which it may be observed that they are of moderate to significant importance with weak hydrogen bonds occurring within the supramolecular synthons I and II (Scheme 2). Several features are common with the 1:1 complex of TNB with dibenzanthracene, whereby synthons III and IV incorporating elements of synthons I and II are present.[34,35] Synthons I and II provide the connectivity between molecules in the crystal. Figure 3 shows the

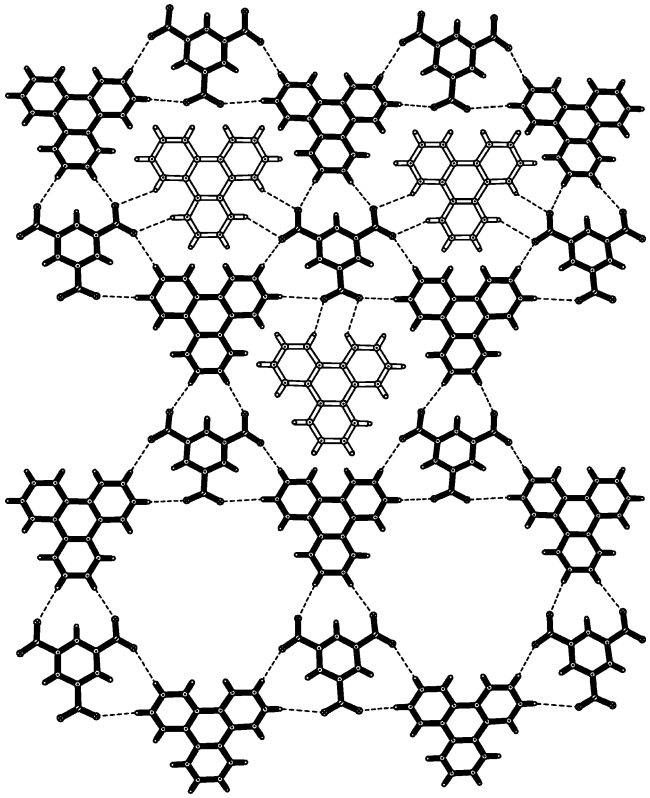

Figure 3. Three-connected honeycomb network of alternating TNB and TP molecules. The molecules are shaded. Dotted lines represent C−H···O hydrogen bonds. The unshaded TP molecules belong to an equivalent interpenetrated network.

immediate environment of TNB and TP molecules in the crystal. Each molecule of TNB is linked to three molecules of TP via synthon I (shaded molecules); in turn, each molecule of TP is connected to three molecules of TNB, and the result is a 3-connected honeycomb network (shaded). Additionally, the reference molecule of TNB is linked to three other TP molecules (unshaded) via synthon II. A consideration of the synthon II linkages leads to an alternative 3-connected honeycomb network.

Any TNB molecule is thus surrounded by six TP molecules, three being linked to it via synthon I and the rest linked via synthon II. Starting with this reference TNB molecule, the structure may be described, with equal validity, in terms of hexagonal honeycomb networks constituted with either synthon I or with synthon II. It should be noted further that the reference TNB molecule and its six immediate neighbors are not within the same plane. The structure is devoid of 2-D trigonal networks, as is required in single component octupolar crystals such as TATB.[16]

More interestingly, the structure may be viewed as a triply interpenetrated network of the archetype honeycomb pattern. Let us consider the synthon-I-mediated network. Figure 4(a) shows how three such networks (yellow, magenta, and cyan) interpenetrate via translation. TNB and TP molecules in adjacent translated networks are related by $\pi-\pi$ stacking interactions and also via the synthon II linkages. Figure 4(b) shows the lateral view and it is seen that the corrugation inherent in the network allows for translational interpenetration.[36] This braided pattern is a familiar feature that has been observed previously. Zaworotko et al. have

(32) Thalladi, V. R.; Panneerselvam, K.; Carrell, C. J.; Carrell, H. L.; Desiraju, G. R. *J. Chem. Soc., Chem. Commun.* **1995**, 341.
(33) Thallapally, P. K.; Chakraborty, K.; Carrell, H. L.; Kotha, S.; Desiraju, G. R. *Tetrahedron* **2000**, *56*, 6721.
(34) Biradha, K.; Nangia, A.; Desiraju, G. R.; Carrell, C. J.; Carrell, H. L. *J. Mater. Chem.* **1997**, *7*, 1111.
(35) Carrell, H. L.; Glusker, J. P. *Struct. Chem.* **1997**, *8*, 141.

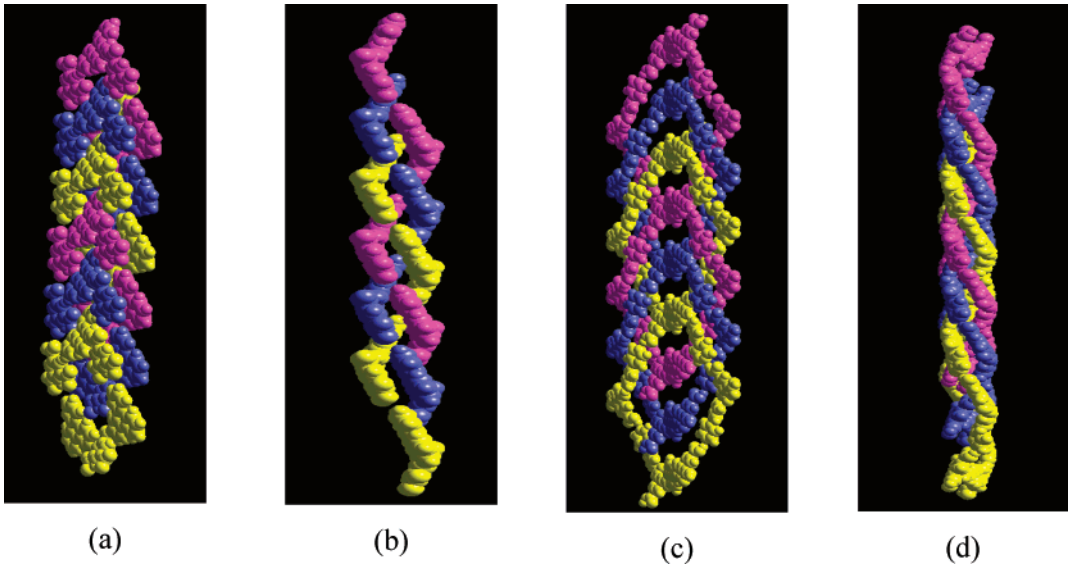

Figure 4. (a) Threefold interpenetration of honeycomb TNB−TP networks in the title complex. (b) Lateral view of (a) to show braiding. (c) Triply interpenetrated arrangement of trimesic acid (benzene-1,3,5-tricarboxylic acid) with 4,4′-bipyridine. Notice the topological similarity to the interpenetration in the title complex. (d) Lateral view of (c) to be compared with (b).

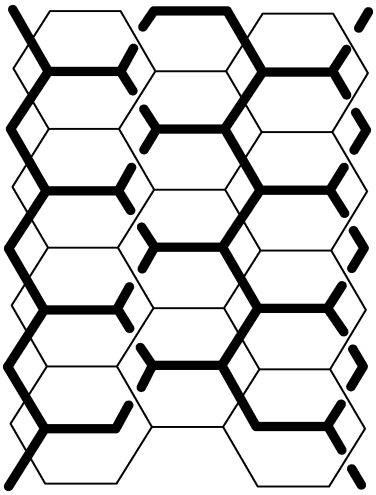

Figure 5. Mode of interpenetration of TNB−TP networks in the title complex (after Robson).

discussed the crystal structure of trimesic acid-4,4′-bipyridine in terms of a honeycomb arrangement of the 3-connected acid molecules, with bipyridine moieties acting as linear spacers.[37] The interpenetrated arrangement is shown in Figure 4(c) and (d) from which the close similarity to the TNB−TP structure may be inferred. A very similar analysis of the title structure is possible if one were to start with the synthon-II-mediated honeycomb network. In this case, molecules in translated and interpenetrated networks would be related by synthon-I-based linkages.

To summarize, the topological consequences of synthons I and II are identical in the structure. Robson has analyzed various interpenetration topologies for 3-connected honeycomb networks.[36] (The interpenetration is shown as 2-fold in keeping with Robson's convention.) Figure 5 shows the arrangement in TNB−TP according to this depiction.

Finally, a structural comparison of TNB−TP and TNB−TMI is pertinent because the crystal optics of the two systems are related in the context of octupolar NLO properties.[38] Certain obvious similarities can be pointed out: both complexes are (a) based on trigonal octupolar molecules; (b) equimolar two-component systems; and (c) noncentrosymmetric; and (d) C−H···O hydrogen bonds are significant in both structures. In TNB−TP, the constituent molecules are interconnected with C−H···O based synthons and there are no discrete layers of TNB and TP. In the latter, however, the constituent TNB and TMI molecules are structurally isolated, occurring in stacked planar layers. Although both crystals promote the D_{3h} symmetry of molecular components into the crystalline level, the major difference is that in TNB−TP the molecular planes are well overlapped for optimal $\pi-\pi$ stacking, whereas in TNB−TMI the interleaving of TNB and TMI molecular planes is such that they are not overlapped (that is, molecules in any given layer sit above or below the corresponding vacancies in the adjacent layer). Such packing precludes any sizable level of intermolecular charge transfer between the different molecular units in TNB−TMI. Moreover, in TNB−TP, both types of molecules lie in the planes corresponding to that of the aromatic rings, opening up the possibility of intraplanar lateral intermolecular charge transfer. More importantly, molecules of the one type sit on top of molecules of the other type, thus entailing the possibility of strong interplane or vertical $\pi-\pi$ charge transfer. The preferred void-filling packing mode of TNB−TMI as opposed to the $\pi-\pi$ vertical stacking in TNB−TP may be due to the steric hindrance resulting from the out-of-plane methyl TMI groups, the planar structure of the TP molecule being more readily compatible with the $\pi-\pi$ vertical interactions.

In general, it is also relevant to mention that the network requirements for centrosymmetry and noncentrosymmetry are distinct for one-component and two-component molecular crystals. According to ref 17, a trigonal (or six-connected) network is compatible with

(36) Batten, S. R.; Robson, R. *Angew. Chem., Int. Ed.* **1998**, *37*, 1460.
(37) Sharma, C. V. K.; Zaworotko, M. J. *Chem. Commun.* **1996**, 2655.

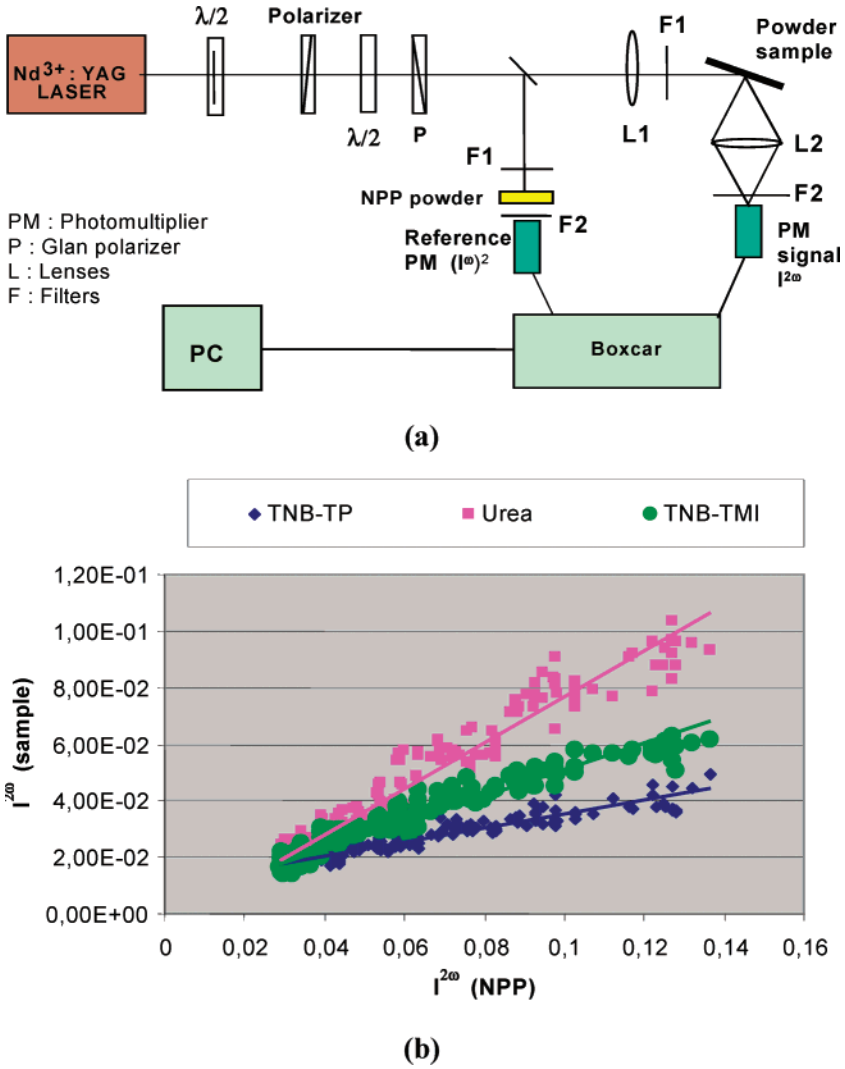

Figure 6. (a) Modified HLS setup for powder test measurements. The powder sample is placed between two parallel glass plates. The incidence angle of the incoming fundamental beam is about 60° with respect to the normal to the glass plates, to eliminate any SHG signal from specular reflection. (b) Plot of the second harmonic emission from urea (squares), TNB−TMI (circles), and TNB−TP (diamonds) with respect to the SHG emission from the reference NPP powder as described in (a). The continuous lines correspond to a linear fit; the corresponding correlation factor exceeds 0.92 in all cases.

noncentrosymmetry whereas a hexagonal (or three-connected) network leads to centrosymmetry. This paradigm has been used widely in the design of octupolar NLO solids.[1,21] However, in two-component crystals such as TNB−TP, 2-D noncentrosymmetric packing is not possible with a trigonal networking, inasmuch as the two components are directly connected in the network. Indeed, under such conditions, a trigonal connectivity is frustrated and is in itself impossible. Rather, a hexagonal network of the type seen in the title compound can and does lead to noncentrosymmetric packing.

Crystal Engineering Analysis of NLO Properties. The TNB−TP 1:1 cocrystal appears in many respects as a uniquely relevant structure for quadratic nonlinear optical properties, building up on the octupolar crystal engineering track seeded by TATB while significantly enlarging its scope. Experimental results will be presented and discussed in terms of effective nonlinear molecular and supramolecular building blocks.

NLO Experimental Results. The semiquantitative Kurtz and Perry SHG powder test has been performed on a finely ground TNB−TP powder. The powdered material was obtained by controlled evaporation of a 1:1 equimolar mixture of TNB and TP from 60:40 benzene/ethanol. Urea has been selected as the benchmarking crystalline material at 1.06 μm. Moreover, the issue of intermolecular H-bonding networks and their influence on molecular crystalline packing in connection with NLO properties is a crucial ingredient common to the currently discussed crystal, as well as to the reference urea crystal, thus providing overall qualitative as well as semiquantitative consistency to a urea-based scale of crystalline NLO efficiency.

The SHG powder test setup basically derives from the harmonic light scattering experiment[3] based on the 90° axis observation of incoherent or partially coherent emission from a statistically disordered sample. A sketch of the setup is shown in Figure 6a, together with a typical plot of the variation of $I^{2\omega}$ with respect to the squared fundamental intensity $(I^{\omega})^2$ (Figure 6b). The $I^{2\omega}$ harmonic signal intensity scales with the square of the "averaged" $\langle\chi^{(2)}\rangle$ (or $\langle d\rangle$) nonlinear tensor and the square of the incoming fundamental intensity according to $I^{2\omega} \approx \langle\chi^{(2)}\rangle(I^{\omega})^2$.

Table 1. Powder Test Results Performed at 1.06-μm Fundamental Wavelength for the Single-Component and Double-Component Crystals[a]

compound	TNB	TP	TNB−TP	TMI	TNB−TMI
$\{I^{2w}\}/\{I^{2w}\}$(urea)	<0.08	0.08	0.3	0.06	0.52
$\{\langle\chi^{(2)}\rangle\}/\{\langle\chi^{(2)}\rangle\}$ (urea)	<0.3	0.3	0.55	0.25	0.72

[a] The methodology followed is described in the text.

The slope is thus defined in arbitrary units with a constant scaling factor related to a diversity of experimental geometrical and sensitivity features. It is normalized to an appropriate SHG signal as from a reference NPP powder. Laser fluctuations are then being averaged and integrated over (typically) 50 pulses. The laser used for fairly transparent compounds as in the present case is a 20-nanosecond-pulse duration Nd^{3+}:Yag laser emitting at 1.06 μm at a 10 Hz repetition rate, with the results being finally referred to urea. Experimental data referring to TNB and TP individual components, the 1:1 complex TNB−TP, pure TMI, and the 1:1 complex TNB−TMI are summarized in Table 1. As already discussed, TNB−TMI is a comparable octupolar 1:1 cocrystal with features similar to that of TNB−TP, however with a major difference in terms of displaced versus superimposed plane-to-plane stacking of the constituent units.

These results clearly confirm the noncentrosymmetric crystal structure of TNB−TP, and further evidence significant enhancement of the nonlinear efficiency of TNB−TP with respect to the pure TP crystal (of the order of KDP powder) whereas the pure TNB crystal does not provide a measurable signal in agreement with its reportedly centrosymmetric packing.[30]

The 1:1 TNB−TMI noncentrosymmetric structure exhibits a signal roughly twice as strong as that from TNB−TP. As in the case of its parent TNB−TP component, the signal from TNB−TMI is significantly stronger than that of the TNB and TMI pure crystals. In both cases, the molecular complex signal is stronger than the sum of the two corresponding native molecule single-crystal signals, thus evidencing the benefit from a cocrystalline engineering strategy, the underlying reasons being rooted in structural or electronic (e.g., charge-transfer-related) features.

At the semiquantitative stage of the powder test experiments (and pending further, more-detailed, ongoing full-fledged single crystal nonlinear experiments) the difference in efficiencies between TNB−TP and TNB−TMI which appears slightly in favor of the latter cannot be fully accounted for. Variations by up to an order of magnitude between averaged $\langle\chi^{(2)}\rangle$ powder values and the actual single crystalline $\chi^{(2)}$ coefficients are not uncommon because of uncertainties in grain-size dispersion, morphology, and the unmonitored absence or occurrence of a phase-matched configuration. Such behavior seems in contradiction with the unoptimized packing of TNB−TMI as compared to TNB−TP entailing weaker $\pi-\pi$ stack intermolecular charge transfer, whereas such a contribution would normally tend to enhance nonlinear effects. Other features may compensate this trend such as the occurrence of more favorable birefringence phase-matched configurations or opposing, and hence mutually balancing, signs for intra- versus intermolecular contributions to $\chi^{(2)}$.

It has become traditional, even in the case of strongly interconnected molecular building blocks, to dissect the overall response in terms of that from individual molecules within a tensorial oriented gas approach.[4] Although such an approach is restricted to averaged Lorenz−Lorentz local field corrections so as to account for intermolecular polarizing effects, it may suffice as a benchmarking model prior to further refinement when eventually needed. It may eventually point out the need to incorporate intermolecular features based on the evidence of otherwise unaccounted for differences between the oriented gas model and actual experimental results. This procedure, which has been applied to organo-mineral crystals[39] or at the molecular scale in the case of nonlinear substituted paracyclophanes,[15] has proved helpful in pointing out strong intermolecular effects, which could not be otherwise accounted for in the framework of a molecular gas model made up of disconnected molecular units.

Octupolar molecules are measured using the incoherent harmonic light scattering technique in solution as pioneered by Maker et al.[3] and more recently revived for octupolar NLO measurements.[3] Experiments were performed in chloroform solutions at varying concentrations in the range of 10^{-2} to 10^{-3} M under increasing incoming fundamental intensities to ascertain the quadratic dependence of the emitted signal intensity with respect to both concentration and fluence parameters. The transparency in the visible range of molecules under investigation allows for the use of a 1.06 μm Nd^{3+}:YAG generated fundamental beam with 20-ns pulse duration at a 10-Hz repetition rate entailing no detectable two-photon fluorescence background otherwise frequently met in the case of more absorbing species.

The geometry of the experiment has been already mentioned in the context of the powder test and has been extensively described elsewhere: it comprises right angle detection of the scattered signal with the possibility of polarizing and analyzing the incoming fundamental and outgoing harmonic beams so as to monitor the nonlinear anisotropy of molecules and infer the quantitative balance between dipolar and multipolar contributions in more general multipolar systems.[19] Such a configuration may eventually confirm the purely octupolar nature of the investigated species in the more symmetric cases. Results for urea, TNB, TP, and TMI are reported in Table 2. Solvents used were water in the case of urea, and chloroform for TNB, TP, and TMI.

Plain application of an oriented gas model taking into account the angular positions of individual molecules in the unit cell has led to the introduction of an intermediary **b** nonlinear tensor[4] accounting for the crystalline nonlinearity per molecule according to the

(38) (a) Thalladi, V. R.; Brasselet, S.; Weiss, H.-C.; Blasér, D.; Katz, A. K.; Carrell, H. L.; Boese, R.; Zyss, J.; Nangia. A.; Desiraju, G. R. *J. Am. Chem. Soc.* **1998**, *120*, 2563. (b) Thalladi, V. R.; Brasselet, S.; Blaser, D.; Boese, R.; Zyss, J.; Nangia, A.; Desiraju. *Chem. Commun.* **1997**, 1841. (c) Filippini, G.; Gavezzotti, A. *Chem. Phys. Lett.* **1994**, *231*, 86. (d) Wortmann, R.; Glania, C.; Krämer, P.; Matschiner, R.; Wolff, J. J.; Kraft, S.; Treptow, B.; Barbu, E.; Längle, D.; Görlitz, G. *Chem. Eur. J.* **1997**, *3*, 1765. (e) Wolff, J. J.; Siegler, F.; Matschiner, R.; Wortmann, R. *Angew. Chem., Int. Ed.* **2000**, *39*, 1436. (f) Cho, B. R.; Park, S. B.; Lee, S. J.; Son, K. H.; Lee, S. H.; Lee, M.; Yoo, J.; Lee, Y. K.; Lee, G. J.; Kang, T. I.; Cho, M.; Jeon, S. J. *J. Am. Chem. Soc.* **2001**, *123*, 6421.

(39) Kotler, Z.; Hierle, R.; Josse, D.; Zyss, J.; Masse, R. *J. Opt. Soc. Am. B* **1992**, *9*, 534.

Table 2. Quadratic Hyperpolarizability Values of Molecules of Interest

compound	β (1.06 μm) in 10^{-30} esu	β_0[a] in 10^{-30} esu	λ_{max}
urea	0.45	0.37	200 nm
TNB	3.3 ± 0.4	2.4 ± 0.3	249 nm
TP	6.2 ± 0.3	4.4 ± 0.2	260 nm
TMI	3.7 ± 0.4	2.8 ± 0.3	242 nm

[a] β_0 Stands for the static hyperpolarizability following dispersion by the two-level quantum model based on the higher level energy from λ_{max}, the maximum absorption wavelength in solution.

following Cartesian expression valid for a two-component cocrystal such as that investigated here:

$$b_{IJK} = \frac{\chi^{(2)}_{IJK}}{NF_{IJK}} = \beta^{A}_{i_A j_A k_A}(\mathbf{I}\cdot\mathbf{i}_A)(\mathbf{J}\cdot\mathbf{j}_A)(\mathbf{K}\cdot\mathbf{k}_A) + \beta jk^{D}_{i_{DDD}}(\mathbf{I}\cdot\mathbf{i}_D)(\mathbf{J}\cdot\mathbf{j}_D)(\mathbf{K}\cdot\mathbf{k}_D) \quad (1)$$

Contrary to $\chi^{(2)}$, **b** is a local field correction free tensor, N is the number of TNB (or TP) molecules per unit volume, β^A (respectively, β^D) stands for the quadratic hyperpolarizability tensor of molecule A (respectively, D), with A and D labeling the two molecular components of the cocrystal (this picture for a two-component cocrystal is strictly equivalent, from NLO related properties, to that of a single component crystal, howeve, with two unrelated molecules in the unit cell as extensively discussed in ref 4).

Finally, index i_A, j_A, and k_A (respectively, i_D, j_D, and k_D) refer to local molecular axes attached to molecule A (respectively, D) and I, J, and K refer to a common set of crystalline axes from a crystalline framework which is obtained by crystal symmetry considerations eventually complemented by additional dielectric polarization considerations for lower crystal symmetry situations as in the case of methyl-amino-propanoate (MAP).[4] Molecular frameworks $\{\mathbf{x}_A,\mathbf{y}_A,\mathbf{z}_A\}$ and $\{\mathbf{x}_D,\mathbf{y}_D,\mathbf{z}_D\}$ have to be connected by crystal point group symmetry operations so as to allow for further evidence of eventual intra-unit cell symmetry that may lead to further **b** or $\chi^{(2)}$ tensor simplifications which are not amenable to the more traditional application of pure crystalline symmetry considerations (see ref 4). A more detailed discussion is provided in Appendix A with a justification for eq 1.

One can further simplify this expression by considering the specific positions of TNB and TP molecules within the unit cell of TNB−TP with label A (respectively, D) for the electron-accepting (respectively, donating) TNB (respectively TP) moiety. We further assume for the sake of simplification that molecules A and D are strictly parallel, which is an approximation valid by less than one degree angular deviation. The three main configurations of interest are depicted in Figure 7 namely an eclipsed, anti-eclipsed, and the more general staggered case with an arbitrary 2θ angle between the two Y-shaped species referred to a natural definition for the {X,Y,Z} framework.

Considerable simplification from the Cartesian formulation of the oriented gas as in eq 1 can be brought about by the irreducible decomposition of the β tensors in a more adequate combined Cartesian−spherical tensor formalism as introduced in ref 16 and further implemented, for example, in ref 40. Assuming additive behavior for the β tensors of subunits A and B leads to the simpler expression eq 2, for the most general case of a staggered stack at an arbitrary θ angular deviation between A and D

$$\beta = \beta_A + \beta_D = \cos(3\theta)(\beta_A + \beta_D)\mathbf{X}\otimes(\mathbf{X}\otimes\mathbf{X} - 3\mathbf{Y}\otimes\mathbf{Y}) + \sin(3\theta)(\beta_A - \beta_D)\mathbf{Y}\otimes(\mathbf{Y}\otimes\mathbf{Y} - 3\mathbf{X}\otimes\mathbf{X}) \quad (2)$$

In the right side of the expression, the β_A (respectively, β_D) notation stands for coefficient β^A_{xxx} (respectively, β^D_{xxx}) so as to simplify notations whereas the β_A (respectively, β_D) shorthand notation in the left side of eq 2 refers to the full quadratic hyperpolarizability tensor of molecule A (respectively, D).

The squared modulus of the β tensor then takes the following expression:

$$\{||\beta^2(\theta)||^2\}/\{4 = (\beta_A + \beta_D)^2\cos^2 3\theta + \} (\beta_A - \beta_D)^2\sin^2 3\theta \quad (3)$$

It is important to note that the possibly misleading 3-integer factors showing up in terms such as $3\mathbf{X}\otimes\mathbf{Y}\otimes\mathbf{Y}$ in eq 2 are of combinatorial origin and are introduced here as a shorthand notation for the more fully developed exact $\mathbf{X}\otimes\mathbf{Y}\otimes\mathbf{Y} + \mathbf{Y}\otimes\mathbf{X}\otimes\mathbf{Y} + \mathbf{Y}\otimes\mathbf{Y}\otimes\mathbf{X}$ tensor sum. Hence, each accompanying β coefficient in the fully developed expression must be individually squared toward the β tensor modulus evaluation as already pointed out in ref 16.

It is clear from eq 3 that the relative sign of β_A and β_D plays an important role in designating the maxima and minima of the β modulus versus θ as shown in the plots of Figure 7. Indeed, when $\beta_A\,\beta_D > 0$, a maximal value of $4(\beta_A + \beta_D)^2$ is reached at any integer multiple of $\pi/3$, thus designating the eclipsed configuration as the optimum. For $\beta_A\,\beta_D < 0$, a maximal value of $4(\beta_A - \beta_D)^2$ is reached at $\pi/6 + m\,\pi/3$ (with m as an arbitrary positive or negative integer) corresponding to the anti-eclipsed configuration.

This model does not provide a full picture to discuss the optimization of the bulk $\chi^{(2)}$ susceptibility at it ignores intermolecular interactions which are prone to take place in view of the compact π-plane to π-plane stacking bringing into close contact, along the a axis, the electron-accepting TNB and electron-donating TP species. Introducing a third Z axis perpendicular to the quasi-parallel planes of the TNB and TP moieties, the full 3-D {**X**,**Y**,**Z**} "bisector" framework allows us to discuss thereafter a more comprehensive interactive model of the bi-molecular stack.

In the noninteracting staggered stack, there remain only two independent coefficients for β, namely in Cartesian notations as from eq 2:

$$\beta_{xxx} = -\beta_{xyy} = \cos 3\theta(\beta_A + \beta_D) \quad (4)$$

$$\beta_{yyy} = -\beta_{yxx} = \sin 3\theta(\beta_A - \beta_D) \quad (5)$$

The interacting stack retains 3-fold symmetry features which will further constrain and simplify tensorial expressions. However, when "branching" interaction along the Z axis, two additional coefficients show up,

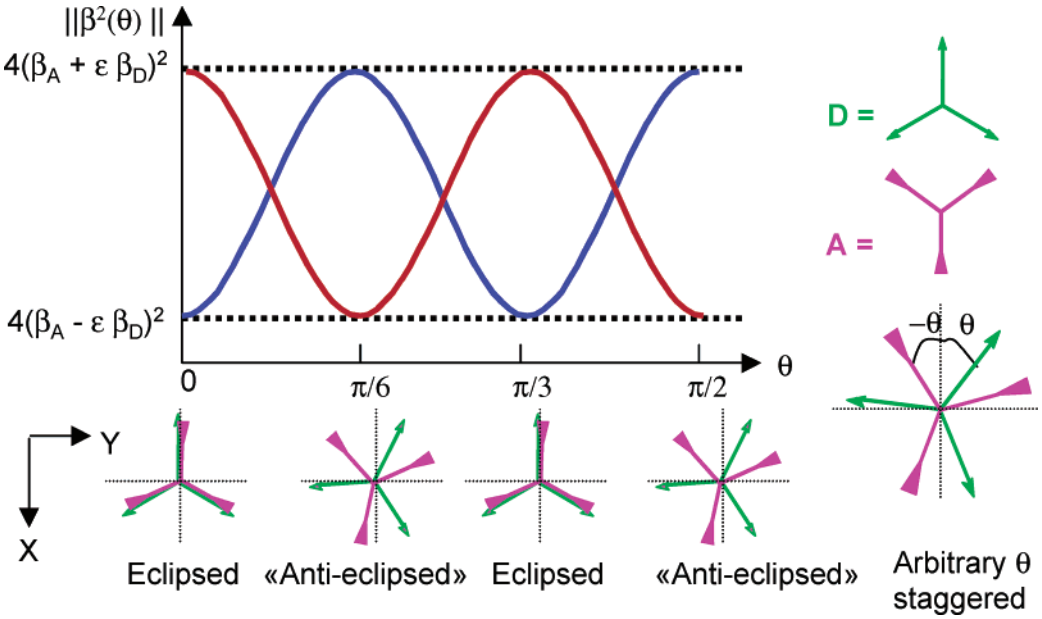

Figure 7. Plot of the square modulus of β as a function of θ for various configurations of a bimolecular parallel stack with trigonal planar subunits A and D; the red (respectively blue) line plot corresponds to $\epsilon = 1$ (respectively $\epsilon = -1$) for $\beta_A.\beta_D > 0$ (respectively < 0).

thus enlarging the number of independent coefficients from two to four, namely:

$$\beta_{zzz}, \beta_{zxx} = \beta_{zyy}, \beta_{xxx} = -\beta_{xyy}, \text{ and } \beta_{yyy} = -\beta_{yxx}$$

Following C_3 symmetry, the four independent coefficients can be rearranged to form the dipolar and octupolar irreducible components of β, namely:

$$\beta_{J=1} = \frac{3}{5}(\beta_{zzz} + 2\beta_{zxx})\mathbf{Z} \otimes (\mathbf{X} \otimes \mathbf{X} + \mathbf{Y} \otimes \mathbf{Y} + \mathbf{Z} \otimes \mathbf{Z}) \quad (6)$$

$$\beta_{J=3} = \beta_{xxx}\mathbf{X} \otimes (\mathbf{X} \otimes \mathbf{X} - 3\mathbf{Y} \otimes \mathbf{Y}) + \beta_{yyy}\mathbf{Y} \otimes (\mathbf{Y} \otimes \mathbf{Y} - 3\mathbf{X} \otimes \mathbf{X}) + \frac{1}{5}(\beta_{zzz} - 3\beta_{zxx})\mathbf{Z} \otimes (2\mathbf{Z} \otimes \mathbf{Z} - 3\mathbf{X} \otimes \mathbf{X} - 3\mathbf{Y} \otimes \mathbf{Y}) \quad (7)$$

The essential consequence of intermolecular interaction is then to lower the point-group symmetry from D_{3h} (from a point-group symmetry viewpoint, a noninteracting stack of 2-D trigonal planar systems amounts to an overall planar system with a 3-fold symmetry axis perpendicular to the common plane) to C_3 with the emergence along Z of a $\beta_{J=1}$ vector part to β (absent in D_{3h} systems) and an additional "Z-containing" off-plane component in $\beta_{J=3}$ as in the last part of eq 7. Although the first part of eq 7, namely

$$\beta_{xxx}\mathbf{X}(\mathbf{X} \otimes \mathbf{X} - 3\mathbf{Y} \otimes \mathbf{Y}) + \beta_{yyy}\mathbf{Y} \otimes (\mathbf{Y} \otimes \mathbf{Y} - 3\mathbf{X} \otimes \mathbf{X})$$

is strictly identical, as far as tensorial symmetry is concerned, to its D_{3h} counterpart expression in eq 2, it may significantly differ in magnitude as the former (respectively, the latter) refers to interacting (respectively, independent) molecular units. Be it in a noninteracting or interacting bimolecular stack picture as accounted for, respectively, by eqs 2 or 6 and 7, the next step is to promote the corresponding β to a crystalline $\chi^{(2)}$ tensor.

To up-scale β from molecular to crystalline levels, the adequate choice of crystalline axis is critical and stands at the outcome of a possibly subtle combination of crystalline and dielectric considerations, as already mentioned. Each crystal is then a specific case and we shall henceforth concentrate on TNB−TP. Like MAP,[4] TNB−TP is a low-symmetry $P2_1$ crystal, albeit with significant differences arising from intracell packing considerations. Contrary to MAP, wherein the two symmetry-related quasi-planar molecules are shaping a dihedron (thus designating the intersection of their average plane as a dispersion-free noncrystallographic principal dielectric axis), the TNB and TP molecules are located in quasi-parallel planes in the case of the TNB−TP lattice. In fact, the TNB−TP crystal structure can be viewed as generally abiding to a quasi-D_{3h} symmetry point group with small structural differences accounting for the actual $P2_1$ space group.

A natural choice for the crystalline dielectric reference frame is then simply {**X**,**Y**,**Z**} as already defined in Figure 7 for the case of an eclipsed stack, with Z along the direction normal to the TNB and TP quasi-parallel planes, X and Y within the plane, and X quasi-parallel to the crystalline 2-fold symmetry axis. The angle between X and the a crystal axis is of the order of 20°. The crystal is negatively quasi-uniaxial with its optical axis along Z and an ordinary index within the π-conjugated molecular {**X**,**Y**} plane significantly higher than its counterpart off-molecular plane extraordinary index along Z. The $\chi^{(2)}$ or **b** tensor (see Appendix A) can then be readily inferred by mere tensorial addition from the β tensor of individual molecular stacks, be it given by eq 2 for independent moieties or eqs 6 and 7 in the more elaborate picture of effectively interacting "dressed" species, namely $b_{IJK} = \chi^{(2)}/NF_{IJK} = \beta_{IJK}$, with β_{IJK} provided by eqs 2 or 7 depending on the choice of the molecular building block.

Note that eq 2 is considerably simplified for a quasi zero θ value, namely:

$$\beta = \beta_{J=3} = (\beta_A + \beta_B)\mathbf{X} \otimes (\mathbf{X} \otimes \mathbf{X} - 3\mathbf{Y} \otimes \mathbf{Y}) \quad (8)$$

whereas eq 7 becomes eq 9 (eq 6 remains unchanged):

$$\beta_{J=3} = \beta_{XXX}\mathbf{X} \otimes (\mathbf{X} \otimes \mathbf{X} - 3\mathbf{Y} \otimes \mathbf{Y}) + \frac{1}{5}(\beta_{ZZZ} - \beta_{ZXX})\mathbf{Z} \otimes (2\mathbf{Z} \otimes \mathbf{Z} - 3\mathbf{X} \otimes \mathbf{X} - 3\mathbf{Y} \otimes \mathbf{Y}) \quad (9)$$

Finally, $b_{J=1} = \beta_{J=1}$ and $b_{J=3} = \beta_{J=3}$, the former occurrence of a vectorial $J = 1$ contribution to **b** and $\chi^{(2)}$ standing out as a signature of $\pi-\pi$ intermolecular interplane interaction. The choice of effective molecular-level building blocks to feed an adequate model capable of accounting for crystalline level optical properties can be further discussed in view of Figure 3. In this figure one can either focus on a TNB (respectively, TP) molecule surrounded by six TP (respectively, TNB) counterpart species making up for a planar supramolecular building block. TNB (respectively, TP) surrounded by six TP (respectively, TNB) entities exemplifies a case of octupolar supramolecular arrangements which echoes, albeit in a different chemical context, the dendritic heptamer aggregate of organometallic octupoles as in ref 41. Such supramolecules can be viewed respectively as "dressed" TNB and TP molecules, the lateral environment of TNB (respectively, TP) by six adjacent TP (respectively, TNB) molecules entailing the possibility of intra-plane intermolecular charge transfer interaction respectively mediated by synthon I and synthon II. In addition to lateral intra-plane CT interactions, stronger "vertical" plane-to-plane $\pi-\pi$ interactions are expected to take place along the *Z* optical axis. Indeed, a more comprehensive picture would consist of considering dressed TNB and TP molecules to feed the interacting stack model leading to eq 7, with the β coefficients referring to a "dressed" bimolecular stack, whereas the cruder benchmark eq 2 expression refers to the simple addition of β_A and β_D tensors in a noninteracting situation.

A quantitative, quantum-chemistry-based analysis of the relevance of these models of increased sophistication when confronted with experimental results is underway and will be presented separately.[42]

As far as applications are concerned, it is noteworthy that propagation along the *Z* axis will provide polarization-independent second harmonic generation and related quadratic nonlinear optical effects. Moreover, such a configuration will allow one to address upfront, at no projection factor cost, the molecular planes whereby the polarizable π-electrons which mediate the nonlinear effects are confined. However, such occurrence of *Z*-indexed off-axis $\chi^{(2)}$ coefficients of possible significance may drastically alter this picture. If the β_{ZZZ} and related $\chi^{(2)}_{ZZZ}$ coefficients prove to be of significance, the most adequate propagation directions to take advantage of such "off-plane" nonlinear polarization mechanism must then be at an oblique angle with respect to the normal to plane direction as discussed in ref 43. This could then favorably impact the crystal overall efficiency due to the possibility of birefringence phase matching which would be otherwise precluded in the absence of *Z*-indexed components when propagating along *Z*.

Conclusion

We have exemplified an octupolar supramolecular cocrystalline engineering scheme involving, besides hydrogen bonding interactions as reported earlier,[38] intermolecular $\pi-\pi$ charge transfer due to an optimal stacking between strongly overlapping molecular subunits. It has also been shown that, contrary to the case of a single compound crystal where a trigonal molecular arrangement is desired and hexagonal packing is forbidden, a cocrystalline scheme involving a couple of different subunits relaxes such centrosymmetry breaking symmetry constraint and allows for a 2-D hexagonal packing. Furthermore, such symmetry lowering from trigonal to hexagonal, while still compatible with noncentrosymmetry in the case of cocrystals, is more in keeping with a general crystallization trend favoring more isotropic structures. Moreover, possibly significant gains in nonlinear efficiency (still to be ascertained on the basis of more theoretical and experimental investigations in the present case of TNB−TP and that of other crystalline structures to be unveiled along the blueprint of TNB−TP) can be expected from intermolecular donor−acceptor charge-transfer interactions beyond the sole and more traditional involvement of intramolecular donor−acceptor interactions.

Powder SHG studies clearly evidence a strong enhancement of the NLO efficiency of TNB−TP with respect to that of pure TP or TNP single-component crystals, thus demonstrating in this case the interest of a cocrystallization scheme for improving the second-order susceptibility of the resulting material. The expected departure from the oriented gas model in octupolar structures such as TNB−TP is discussed within a tensorial framework, where the occurrence of a vectorial $J = 1$ contribution to $\chi^{(2)}$ would be the signature of $\pi-\pi$ interplane interactions. Such a "through-space" charge transfer between 2D conjugated units has been already pointed out and discussed, both theoretically and experimentally, in the case of a family of multiply substituted paracyclophane derivatives.[15] In a similar perspective, further investigations of TNB−TP are currently under progress, involving both solid-state quantum chemistry modeling and experimental NLO studies of $\pi-\pi$ through-space charge transfer processes in both solutions and crystals. Moreover, synthetic implementation of other crystalline engineering schemes remains highly desirable so as to further materialize and refine some of the considerations proposed here.

Appendix A

Crystallographic data and the accompanying refinement features are detailed in Tables 3 and 4.

(40) Andraud, C.; Zabulon, T.; Collet, A.; Zyss, J. *Chem. Phys.* **1999**, *245*, 243.

(41) Le Bozec, H.; Le Bouder, T.; Maury, O.; Bondon, A.; Ledoux, I.; Deveau, S.; Zyss, J. *Adv. Mater.* **2001**, *22*, 1677. Dhenaut, C.; Ledoux, I.; Samuel, I.; Zyss, J.; Bourgault, M.; Le Bozec, H. *Nature* **1995**, *374*, 339.

(42) Zyss, J.; Berthier, G. *J. Chem. Phys.* **1982**, *77*, 3635. Rérat, M.; Zyss, J. Work in progress.

(43) Zyss, J.; Brasselet, S.; Thalladi, V. R.; Desiraju, G. R. *J. Chem. Phys.* **1998**, *109*, 658.

(44) Zyss, J.; Boulanger, B. In *International Tables for Crystallography, Volume D Physical Properties*; Authier, A., Ed., Kluwer: Boston, MA, In press 2003.

Table 3. Crystallographic Data

	TNB−TP
empirical formula	$(C_{12}H_{12})\cdot(C_6H_3N_3O_6)$
formula wt.	441.39
crystal system	monoclinic
space group	$P2_1$
CCDC No.	176990
a [Å]	7.1488(4)
b [Å]	8.661(5)
c [Å]	16.3094(9)
β [°]	97.780(1)
Z	2
volume [Å^3]	1003.64(10)
D_{calc} [g/cm^3]	1.461
μ [mm^{-1}]	0.107
θ [°]	1.28−28.47

Table 4. Structural Refinement Parameters

range of h k l	$-9 \le h \le 9$ $-11 \le k \le 11$ $-21 \le l \le 21$
$F(000)$	456
parameters	298
reflns. collected	11427
unique reflns.	4874
observed reflns.	2198
R_1 [$I > 2\sigma(I)$]	0.0681
WR_2 [all]	0.1560
diffractometer	Siemens SMART CCD

Appendix B

We recall hereafter the basic ingredients of the oriented gas model, albeit in a more compact tensorial form allowing for the convenient introduction of the contraction operator for tensorial coupling (notation •). The crystal consists of two molecules per unit cell, namely A and D with their respectively attached β_A and β_D NLO tensors defined in the corresponding $\{\mathbf{x}_A,\mathbf{y}_A,\mathbf{z}_A\}$- and $\{\mathbf{x}_D,\mathbf{y}_D,\mathbf{z}_D\}$ local molecular frameworks. The related $i_{A,D}$ vectorial variables and $i_{A,D}$ index running over the three $\mathbf{x}_{A,D}$, $\mathbf{y}_{A,D}$ and $\mathbf{z}_{A,D}$ directions attached to the A or D local frameworks will be used.

In the comprehensive principal dielectric framework $\{\mathbf{X},\mathbf{Y},\mathbf{Z}\}$ (which may not fully coincide with the crystalline framework in the case of low-symmetry systems), the **b** tensor is defined as the local-field correction free-crystalline quadratic tensor per unit cell with coefficients related to the usual $\chi^{(2)}$ tensor by[4]

$$\chi^{(2)}_{IJK} = NF_{IJK} \times \mathbf{b}_{IJK} \qquad \text{(B1)}$$

$N = {}^1/_V$ where V stands for the unit cell volume, F_{IJK} is the overall local field correction tensor defined as $f_I^{2\omega} f_J^{\omega} f_K^{\omega}$ in terms of Lorenz−Lorentz factors and $f_I^{\omega,2\omega} = [(n_I^{\omega,2\omega})^2 + 2]/3$ with I, J, and K running over the X, Y, Z directions of the principal dielectric tensor.

In the following typical tensorial expressions, Einstein's convention for implicit summation of repeated indices is used, namely:

$$b = \sum_{I,J,K} \mathbf{b}_{IJK}\mathbf{I} \otimes \mathbf{J} \otimes = \mathbf{b}_{IJK}\mathbf{I} \otimes \mathbf{J} \otimes \mathbf{K} \qquad \text{(B2)}$$

As formalized in ref 44 the $\chi^{(2)}$ [and **b**] tensors can be further contracted with a field tensor $\mathbf{D} = \mathbf{d}_{2\omega} \otimes \mathbf{d}_{\omega} \otimes \mathbf{d}_{\omega}$ to generate the induced polarization along the $\mathbf{d}_{2\omega}$ transverse unit vector whereas $\mathbf{d}_{\omega}$ stands for the corresponding transverse unit vector along the incoming fundamental polarization. We refer here to the transverse displacement D field rather than to the E electric field so as to be able to discard eventual walk-off angular factors that might otherwise uselessly obscure the following discussion.

Such induced harmonic polarization can be either ordinary or extraordinary and may thus be accordingly labeled as $\mathbf{P}_o$ or $\mathbf{P}_e$ depending on the specific ordinary or extraordinary nature of the incoming fundamental polarizations as well as on the nonzero $\chi^{(2)}$ tensorial terms which have not vanished upon imposition of crystal symmetry constraints and are enabling effective light matter coupling. The following compact expression then fully embodies light-matter quadratic nonlinear interaction

$$P = \chi^{(2)}\bullet D \qquad \text{(B3)}$$

where we have left out the (o, e) notation for the sake of simplicity (in the case of propagation along the principal axis, such omission is valid as all fields are then along the other principal axis thus canceling walk-off).

Finally, expressions B4 and B5 readily lead to B6 to provide a unifying link between crystalline **b** tensor and the β hyperpolarizability of individual molecules, thus eventually allowing us to consistently relate molecular properties to the macroscopic induced polarization via additional use of B1 and B3.

$$\mathbf{b}_{IJK} = \mathbf{I} \otimes \mathbf{J} \otimes \mathbf{K}\bullet(\boldsymbol{\beta}^A + \boldsymbol{\beta}^D) \qquad \text{(B4)}$$

$$\mathbf{b}_{IJK} = \mathbf{I} \otimes \mathbf{J} \otimes \mathbf{K}\bullet(\beta^{\mathrm{A}}_{i_{\mathrm{A}}j_{\mathrm{A}}k_{\mathrm{A}}}\mathbf{i}_{\mathrm{A}} \otimes \mathbf{j}_{\mathrm{A}} \otimes \mathbf{k}_{\mathrm{A}} + \beta^{\mathrm{D}}_{i_{\mathrm{D}}j_{\mathrm{D}}k_{\mathrm{D}}}\mathbf{i}_{\mathrm{D}} \otimes \mathbf{j}_{\mathrm{D}} \otimes \mathbf{k}_{\mathrm{D}}) \qquad \text{(B5)}$$

$$\mathbf{b}_{IJK} = \beta^{\mathrm{A}}_{i_{\mathrm{A}}j_{\mathrm{A}}k_{\mathrm{A}}}(\mathbf{I}\cdot\mathbf{i}_{\mathrm{A}})(\mathbf{J}\cdot\mathbf{j}_{\mathrm{A}})(\mathbf{K}\cdot\mathbf{k}_{\mathrm{A}}) + \beta^{\mathrm{D}}_{i_{\mathrm{D}}j_{\mathrm{D}}k_{\mathrm{D}}}(\mathbf{I}\cdot\mathbf{i}_{\mathrm{D}})(\mathbf{J}\cdot\mathbf{j}_{\mathrm{D}})(\mathbf{K}\cdot\mathbf{k}_{\mathrm{D}}) \qquad \text{(B6)}$$

Molecules A and D may or may not be related by an intramolecular symmetry operation as discussed in ref 4. In the former case, eq B6 can be further simplified to make room for tensorial relations between **b** or $\chi^{(2)}$ coefficients. Such simplifications indded take place in the current interest whereby molecules A and D lie in quasi-parallel planes. These simplifications are indeed borne out in the case of 2-D octupolar stacks by the introduction of an intermediary "bisector" reference axis $\{\mathbf{X},\mathbf{Y},\mathbf{Z}\}$ allowing one to connect $\{\mathbf{x}_A,\mathbf{y}_A,\mathbf{z}_A\}$ and $\{\mathbf{x}_D,\mathbf{y}_D,\mathbf{z}_D\}$ along the lines of ref 4. However, this occurs in a different and more symmetric packing geometry for TNB−TP in comparison with that of MAP (parallel planes in TNB−TP versus intersecting planes for the two molecules in the MAP crystal unit cell).

CM031018M